Arsenic Flux Dependence of Island Nucleation on InAs(001)

Frank Grosse,[1,2] William Barvosa-Carter,[1] Jenna Zinck,[1] Matthew Wheeler,[1] and Mark F. Gyure[1]
[1] *HRL Laboratories LLC, 3011 Malibu Canyon Road, Malibu, California 90265*
[2] *Department of Mathematics, University of California, Los Angeles, California 90095-1555*
(Received 15 May 2001; published 26 August 2002)

The initial stages of InAs(001) homoepitaxial growth are investigated using a combination of kinetic Monte Carlo simulations based on *ab initio* density functional theory and scanning tunneling microscopy. In the two dimensional island nucleation mode investigated, the island number density is found to decrease with increasing As. This behavior is explained by a suppression of the effective In-adatom density leading to a reduction in island nucleation. The relevant microscopic processes responsible for this reduction are identified.

DOI: 10.1103/PhysRevLett.89.116102 PACS numbers: 68.55.–a, 68.37.Ef, 81.15.Aa, 81.15.Hi

The III-V semiconductor compounds are not only of profound technological importance, but the relative simplicity of their growth by molecular beam epitaxy (MBE) has also enabled many well-controlled experimental and theoretical investigations. GaAs, in particular, has become the prototypical material system for investigating the inherent complexities associated with MBE growth of a multicomponent system [1–5]. Nevertheless, very little is understood about the microscopic growth mechanisms of the arsenide family of materials. For example, the basic steps in the nucleation process of islands on the (001) surfaces have only recently received serious attention [3–5]. This lack of understanding makes it difficult to utilize new growth techniques to improve device quality.

Subtle, but clearly observable, changes in growth morphology have been observed in the transition from island nucleation to step flow growth [2,6,7] as a function of As flux for both GaAs and InAs. These experiments indicate that increasing As flux generally enhances step flow growth. Submonolayer island density experiments performed on GaAs show that the island density decreases with As flux [8]; comparable data for InAs, presented in this Letter, show the same trend. These results are not adequately explained by any existing theory. For instance, applying arguments derived from single-component models leads to contradictions: Nucleation theory [9] suggests that the metal diffusivity increases with increasing As flux, whereas intuitively the diffusivity should decrease. The extension of basic thermodynamic arguments to growth [10] suggests a modification of single-component kinetic Monte Carlo (KMC) growth models [2,11]. However, this leads to trends in simulation that are opposite to those observed experimentally for island density and step flow transition temperature [12]. Furthermore, although combined experimental and theoretical investigations [13–15] have led to a deeper understanding of *static* III-V semiconductor surfaces, the basic nucleation mechanisms relevant during *growth* are still controversial. Itoh *et al.* [3] utilized an empirical KMC model for GaAs(001) that, for the first time, included the $\beta2(2\times4)$ reconstruction and found that nucleation starts on the top As-dimer rows. This is in contradiction to recent theoretical predictions that growth is initiated in the $\beta2(2\times4)$ trenches [4,5]. Neither approach has yet been shown to explain the As-flux dependence of island nucleation.

In this Letter, we show that the experimentally observed decrease in island density with increasing As flux on $\beta2(2\times4)$ reconstructed InAs(001) originates in the suppression of one of the key steps in the nucleation process and not from enhanced diffusivity or a decrease in adatom density as previous theories suggest. To identify the specific microscopic processes responsible for island nucleation, we employ a two species KMC model for the growth of InAs that is constrained by input from extensive *ab initio* density functional theory (DFT) calculations and supplemented by experimental data [16]. We present scanning tunneling microscopy (STM) data for submonolayer island densities at different As fluxes and find good agreement with the model predictions.

Our *ab initio* DFT-based KMC simulation treats both species In and As on a zinc blende lattice. The basic processes included are In deposition and diffusion and As_2 deposition and desorption. The In deposition is modeled by adding atoms at randomly chosen surface sites; As-dimer adsorption also occurs randomly but is allowed only on sites where the formation of four dimer-In bonds is possible. Sites with lower coordination are not stable for As dimers within the growth region investigated here. Adhering closely to the framework of transition state theory, we describe In diffusion and As_2 desorption as thermally activated processes where the activation energy is calculated as the difference between a transition and bond energy. All bond energies are determined directly from DFT calculations [17,18] and completely describe the thermodynamics of the surface within the experimentally relevant $\alpha2(2\times4)-\beta2(2\times4)$ reconstruction region [15]. The kinetic parameters, i.e., transition energy and prefactor, are approximated by a constant per species. Our model has been shown [19] to include the thermodynamic stability of the two growth-relevant reconstructions,

 © 2002 The American Physical Society

$\alpha 2(2\times 4)$ and $\beta 2(2\times 4)$. Further details of the KMC model, including a full description of all microscopic processes and parameter determination, will be published elsewhere [16]. Here we describe only the processes and parameters relevant for explaining the dependence of island nucleation on As flux.

To investigate island nucleation experimentally, InAs(001) $-\ \beta 2(2\times 4)$ surfaces are prepared by the following procedure to achieve a flat, well-ordered reconstructed surface before initialization of submonolayer growth. First a buffer layer of 10 monolayer (ML) at $T = 470\,^{\circ}\mathrm{C}$, F(As) = 5 ML/s (determined by the uptake method [20]) and a growth rate F(In) = 0.1 ML/s is grown using a modified VG 80H growth chamber [7] on an existing undoped buffer layer ($>0.5\ \mu$m thick). After stopping the growth, the sample is cooled to $T = 380\,^{\circ}\mathrm{C}$ at a rate of 5°/min, maintaining the original As flux. To heal out growth defects the surface is annealed for an additional 10 min using F(As) = 0.5 ML/s. Then submonolayer growth [T = 380 °C, F(In) = 0.073 ML/s, growth time $t = 2$ s] is initiated at different As fluxes. For investigation by STM, all samples are quenched by simultaneously shutting off the substrate heater power, closing the As_2 and In shutters and the valve on the As_2 source, and rotating the sample towards the cryopanel. Surface morphology and real space reconstruction information are subsequently measured at room temperature using an Omicron LS full-wafer STM.

In Fig. 1(a) we show an STM image of a surface after deposition of 0.15 ML of InAs at F(As) = 2.5 ML/s. Clearly observable are the double As-dimer rows on the terraces pointing along the $[\bar{1}10]$ direction, indicating that the $\beta 2(2\times 4)$ reconstruction is stable under these growth conditions. Nucleated islands are elongated in the $[\bar{1}10]$ direction and are already partially reconstructed. Also observable are smaller structures showing no reconstruction. Using identical growth parameters we carry out KMC simulations starting with a perfect $\beta 2(2\times 4)$ singular surface. The resulting simulated morphology is presented in Fig. 1(b) for a 128×128 lattice. The anisotropy and size of islands given by the simulation correlate well to experiment. We observe that trenches of the reconstruction are free of In atoms.

To compare the As-flux trends between theory and experiment quantitatively, we determine the island densities in experiment and simulation. The resulting numerical values are shown in Table I for different As fluxes. The island number densities in both theory and experiment decrease with increasing As flux. The theoretical island densities are determined from a single run by counting every closed area containing more than 16 In atoms on top of the As-dimer rows as an island. Regions on neighboring dimer rows belong to the same island if the trench between the two is (at least) filled with In atoms. The statistics are checked by comparing to results obtained on lattices with 256×256 sites; no significant change in island density is observed. Identical methods are applied when counting islands in the STM images. The island density is higher in simulation by roughly a factor of 2.

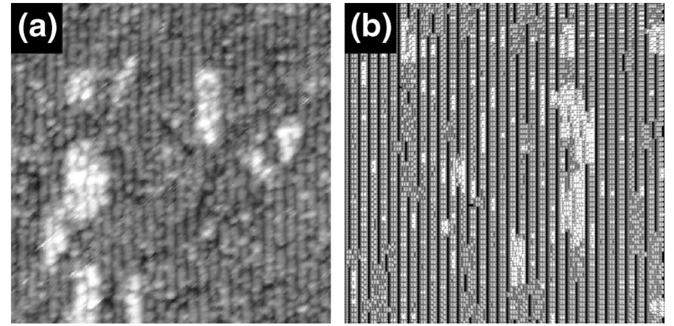

FIG. 1. (a) Filled-state constant current STM image (2 V bias, 0.1 nA) of an InAs(001) surface after 2 s growth at 380 °C, F(As) = 2.5 ML/s, F(In) = 0.073 ML/s, size: 55 nm × 55 nm. (b) Surface morphology in KMC under identical conditions and identical size.

Uncertainties in the experimental determination of temperature, flux, island count, as well as quench effects have been controlled as much as possible but could cause an error in the island density up to approximately 20%. Furthermore, our assumption of a single transition energy for the diffusion of In atoms and single prefactors for each species does not describe the processes exactly. Simulations show that the observed island density trend is robust to numerical changes in, and even reduction of, the model parameter set. Another crucial issue is the physical identity of the As flux measured experimentally with the uptake method [20] compared to the flux of As dimers to the surface used in the simulation. They are identical only if the sticking coefficient of As dimers on the metal rich InAs(001) surface is unity and adsorbed As dimers do not diffuse on InAs(001). Both of these effects, if present, would suggest that a higher As flux should be used in the simulation. Nevertheless, we compare identical As fluxes in Table I and note that an increase by less than an order of magnitude in the simulated flux would bring the measured and simulated island density in quantitative agreement.

The predictive capability of the KMC simulation now allows us to investigate the specific microscopic processes responsible for the experimentally observed As-flux trend. Figure 2 depicts a number of possible situations in the initial nucleation phase with the focus on two main pathways for island formation. Nucleation can be initiated either in the reconstruction trenches or on top of the As-dimer rows. No adsorption of additional As dimers is possible on the initial $\beta 2(2\times 4)$ reconstruction [Fig. 2(a)]. DFT calculations show that, while sites in the

TABLE I. Experimental and simulated island densities with varying As flux at 15% coverage. For other growth conditions, see Fig. 1 and the text.

F(As) (ML/s)	0.15	0.5	2.5	7.5
Experiment (μm^{-2})	5600	4100	2500	
Simulation (μm^{-2})	7400	7400	4400	4000

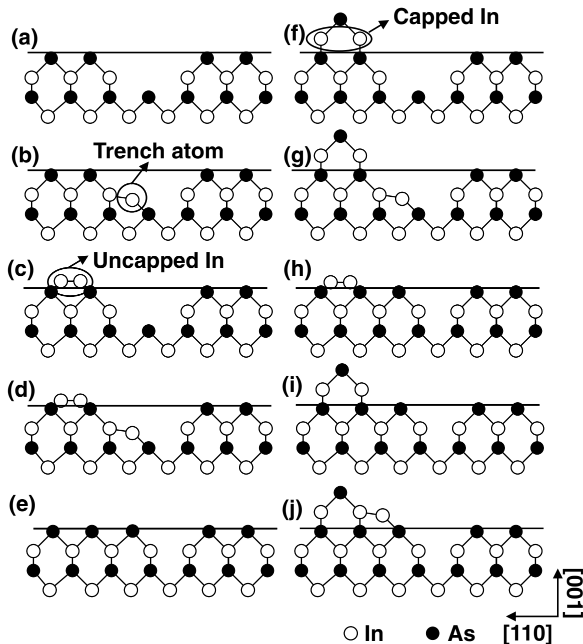

FIG. 2. Schematics of different stages of initial growth on $\beta2(2 \times 4)$ reconstructed InAs(001).

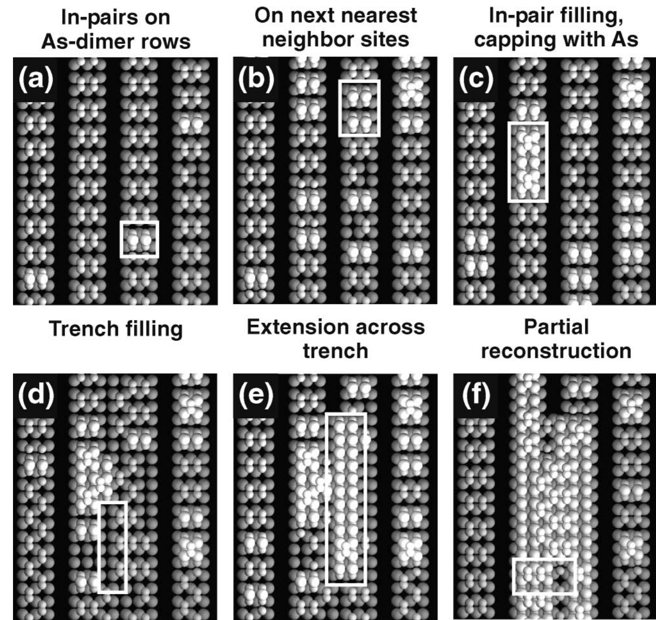

FIG. 3. Simulated formation of islands at different coverages. For growth conditions, see Fig. 1 and the text. Morphology after (a) 0.5 s, (b) 1.0 s, (c) 1.5 s, (d) 1.8 s, (e) 2.0 s, and (f) 2.0 s with simulated quenching.

reconstruction trench for single In atoms [Fig. 2(b)] are energetically favorable, In pairs have the lowest energy forming a [110] bond on top of the As-dimer rows [Fig. 2(c)]. The following possibilities for island nucleation exist depending on the detailed kinetics of As incorporation and the mobility of In. For low As flux, In atoms at a certain coverage will occupy sites on the dimer rows and in the trench [Fig. 2(d)]. The adsorption of As dimers is possible on sites with an existing square arrangement of four In atoms. If the In mobility is low with respect to the As flux, In atoms will be capped in the $\beta2(2 \times 4)$ reconstruction trench [Fig. 2(e)] before they can form pairs on the As dimer rows. The adsorption of As dimers in the trench also needs only two additional In atoms because the $\beta2(2 \times 4)$ trench already provides two bonds. The adsorption of additional As dimers on the dimer rows needs at least four In atoms to provide the necessary bonds [Fig. 2(f)]. If In atoms provide sites for As adsorption in the trench and on the dimer rows [Fig. 2(d)], the remaining steps are given by Fig. 2(g) (adsorption on dimer rows), Fig. 2(h) (adsorption in trench), and Fig. 2(i) (both). After capping the In atoms filling the trench, an extension of the next layer nucleation is possible with additional In. To decide which pathway is the most relevant one, either *nucleation in the trench* [Figs. 2(a), 2(b), 2(e), and 2(h)–2(j) in succession] or *nucleation on the As-dimer rows* [Figs. 2(a), 2(c), 2(f), 2(g), 2(i), and 2(j) in succession], we analyze our KMC simulations.

In Fig. 3, we present a series of pictures showing the time evolution of island formation in the simulation. Deposited In atoms initially occupy sites in the $\beta2(2 \times 4)$ reconstruction trenches followed by formation of In pairs on the As-dimer rows [Fig. 3(a)]. They occupy positions where they break the As dimers and are nearly randomly distributed across the surface. With further increase in coverage, pairs subsequently form on next nearest neighbor sites [Fig. 3(b)]. In pairs can also break up again, however. The remaining two empty sites between two In pairs on next nearest neighbor sites are filled next and, finally, the In on the As-dimer rows is capped with As dimers [Fig. 3(c)]. In the next step the trenches fill with In atoms that are subsequently capped with As dimers [Fig. 3(d)]. The filled trench is bridged to the neighboring As-dimer rows by further In atoms [Fig. 3(e)]. Finally, if the width of In already capped by As dimers on the next layer exceeds the periodicity of the $\beta2(2 \times 4)$ reconstruction, a trench is formed. The islands on the next layer are already partially reconstructed at 15% coverage [Fig. 3(f)].

To elucidate the effect of As flux on the microscopic morphology, we present in Fig. 4 the amount of In occupying sites on the top of the As-dimer rows as a function of time during the simulation. The height level above which In atoms are counted is shown in Fig. 2 for the various structures relevant to the nucleation process. In Fig. 4, no distinction is made between In atoms that are capped [Fig. 2(f)] or uncapped [Fig. 2(c)] by As on the As-dimer rows. The difference between the actual coverage and the number of In atoms on the dimer rows is equal to the amount of In atoms occupying reconstruction trench sites [Fig. 2(b)]. Whereas initially the trench occupation is constant in time and independent of the As flux, at later stages less In is available to form pairs on the As-dimer rows at higher As flux. This is due to the higher probability of capping In atoms with As dimers in the trench [compare Figs. 2(d) and 2(h)]. *Because island nucleation starts on*

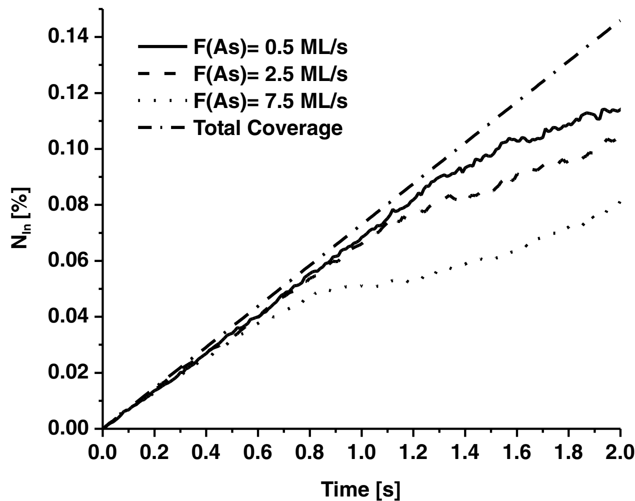

FIG. 4. Time dependent occupation of the top As-dimer rows under different As fluxes.

the As-dimer rows, the reduction of In-adatom density on these rows at higher As flux reduces the number of initial nuclei.

This result can be traced back to the series of microscopic processes responsible for island nucleation. The growth process begins with single In atoms occupying sites in the trench which are 270 meV lower in energy than in equivalent positions atop the dimer rows [Fig. 2(b)]. In pairs, however, have a lower energy on the As-dimer rows [Fig. 2(c)] than in the trench by 870 meV. Only the high mobility of In atoms ensures that In pairs can form on the As-dimer rows before they get capped by As in the trench. Because the As kinetics is slow by comparison [19], the time scales for In atoms and As dimers are decoupled. The high In mobility leads also to a behavior close to thermodynamic equilibrium for adatoms. Therefore, only the bond energies for In atoms are relevant. With increasing As flux, however, more and more In atoms remain initially in the trench and therefore reduce the number of In pairs on the As-dimer rows, which determines the island density at a later stage of the growth. Because of the repulsive interaction between In pairs (-1550 meV), next nearest neighbor sites are initially occupied by In pairs (attractive 80 meV), followed by the nearest neighbor In pair, resulting in a stable complex of six In atoms. The density of In atoms in the trench serves as a site for single As dimers; hence the As flux directly controls the In-adatom density available for nucleation. Because As dimers filling the trench are only sufficiently stabilized by neighboring In atop the dimer rows [compare Figs. 2(e) and 2(h)], growth across the trench is delayed in comparison to growth along the dimer rows resulting in the observed anisotropy of the islands. The remaining In atoms on top are eventually capped by As dimers [Figs. 2(f), 2(g), and 2(j)] and further In atoms are added [Fig. 2(i)]. We observe a considerable reduction in the anisotropy of islands along the dimer rows with increasing As flux that is also directly connected to the observed change in island density. The lower the As flux, the less likely the capping of In in the trenches and therefore the less likely the growth of islands perpendicular to the As-dimer rows.

The arguments used here are also applicable to trends in island to step flow mode transitions (here, for A steps). With increasing As flux the likelihood to cap In atoms in the trench increases leading to faster step advancement and therefore reduced critical temperature, in agreement with experimental results [2,6,7].

We gratefully acknowledge stimulating discussions with P. Kratzer, R. S. Ross, J. Tersoff, and D. D. Vvedensky. This work is supported by NSF and DARPA through Cooperative Agreement No. DMS-9615854 as part of the Virtual Integrated Prototyping Initiative.

[1] S. V. Ghaisas and A. Madhukar, Phys. Rev. Lett. **56**, 1066 (1986).
[2] T. Shitara, D. D. Vvedensky, M. R. Wilby, J. Zhang, J. H. Neave, and B. A. Joyce, Phys. Rev. B **46**, 6815 (1992).
[3] M. Itoh, G. R. Bell, A. R. Avery, T. S. Jones, B. A. Joyce, and D. D. Vvedensky, Phys. Rev. Lett. **81**, 633 (1998).
[4] P. Kratzer, C. G. Morgan, and M. Scheffler, Phys. Rev. B **59**, 15 246 (1999).
[5] P. Kratzer and M. Scheffler, Phys. Rev. Lett. **88**, 036102 (2002).
[6] H. Toyoshima, T. Shitara, P. N. Fawcett, J. Zhang, J. H. Neave, and B. A. Joyce, J. Appl. Phys. **73**, 2333 (1993).
[7] J. H. G. Owen, W. Barvosa-Carter, and J. J. Zinck, Appl. Phys. Lett. **76**, 3070 (2000).
[8] H. Yang, V. P. LaBella, D. W. Bullock, and P. M. Thibado, J. Vac. Sci. Technol. B **17**, 1778 (1999).
[9] J. Venables, *Surface and Thin Film Processes* (Cambridge University Press, Cambridge, U.K., 2000).
[10] J. Tersoff, M. D. Johnson, and B. G. Orr, Phys. Rev. Lett. **78**, 282 (1997).
[11] P. Smilauer and D. D. Vvedensky, Phys. Rev. B **48**, 17 603 (1993).
[12] W. Barvosa-Carter, M. F. Gyure, and F. Grosse (to be published).
[13] W. Barvosa-Carter, A. S. Bracker, J. C. Culbertson, B. Z. Nosho, B. V. Shanabrook, L. J. Whitman, H. Kim, N. A. Modine, and E. Kaxiras, Phys. Rev. Lett. **84**, 4649 (2000).
[14] V. P. LaBella, H. Yang, D. W. Bullock, P. M. Thibado, P. Kratzer, and M. Scheffler, Phys. Rev. Lett. **83**, 2989 (1999).
[15] C. Ratsch, W. Barvosa-Carter, F. Grosse, J. H. G. Owen, and J. J. Zinck, Phys. Rev. B **62**, R7719 (2000).
[16] F. Grosse and M. F. Gyure, Phys. Rev. B **66**, 075320 (2002).
[17] M. Fuchs and M. Scheffler, Comput. Phys. Commun. **116**, 1 (1999).
[18] M. Bockstedte, A. Kley, J. Neugebauer, and M. Scheffler, Comput. Phys. Commun. **107**, 187 (1997).
[19] F. Grosse, W. Barvosa-Carter, J. J. Zinck, and M. F. Gyure, Phys. Rev. B **66**, 075321 (2002).
[20] J. H. Neave, B. A. Joyce, and P. J. Dobson, Appl. Phys. A **35**, 179 (1984).